A new high-temperature multinuclear-magnetic-resonance probe and the self-diffusion of light and heavy water in sub- and supercritical conditions

AUTHOR(S):

Yoshida, K; Wakai, C; Matubayasi, N; Nakahara, M

THE JOURNAL OF CHEMICAL PHYSICS **123**, 164506 (2005)

A new high-temperature multinuclear-magnetic-resonance probe and the self-diffusion of light and heavy water in sub- and supercritical conditions

Ken Yoshida, Chihiro Wakai, Nobuyuki Matubayasi, and Masaru Nakahara[a)]
Institute for Chemical Research, Kyoto University, Uji, Kyoto 611-0011, Japan

(Received 9 June 2005; accepted 16 August 2005; published online 26 October 2005)

A high-resolution nuclear-magnetic-resonance probe (500 MHz for ^{1}H) has been developed for multinuclear pulsed-field-gradient spin-echo diffusion measurements at high temperatures up to 400 °C. The convection effect on the self-diffusion measurement is minimized by achieving the homogeneous temperature distributions of ±1 and ±2 °C, respectively, at 250 and 400 °C. The high temperature homogeneity is attained by using the solid-state heating system composed of a ceramic (AlN) with high thermal conductivity comparable with that of metal aluminium. The self-diffusion coefficients D for light (^1H_2O) and heavy (^2H_2O) water are distinguishably measured at subcritical temperatures of 30–350 °C with intervals of 10–25 °C on the liquid-vapor coexisting curve and at a supercritical temperature of 400 °C as a function of water density between 0.071 and 0.251 g/cm^3. The D value obtained for ^1H_2O is 10%–20% smaller than those previously reported because of the absence of the convection effect. At 400 °C, the D value for ^1H_2O is increased by a factor of 3.7 as the water density is reduced from 0.251 to 0.071 g/cm^3. The isotope ratio $D(^1H_2O)/D(^2H_2O)$ decreases from 1.23 to ~1.0 as the temperature increases from 30 to 400 °C. The linear hydrodynamic relationship between the self-diffusion coefficient divided by the temperature and the inverse viscosity does not hold. The effective hydrodynamic radius of water is not constant but increases with the temperature elevation in subcritical water. © *2005 American Institute of Physics*. [DOI: 10.1063/1.2056542]

I. INTRODUCTION

Recently, super- and subcritical water attracts much attention as a novel and clean solvent that freely dissolves nonpolar organic compounds. Various kinds of new organic reactions have been found to be induced in super- and subcritical water.[1–16] Owing to the characteristic hydration in supercritical water, organic reactions in it can be controlled without a catalyst by tuning an inhomogeneous and anisotropic structure around the solutes. For designing supercritical reactions, it is necessary to understand the dynamic properties of water in the expanded and less packed region; diffusion, dehydration, and collision of reactive species are to be investigated. Especially, the translational diffusion is important since reactive species cannot collide with each other without diffusion. However, the method to observe translational dynamics in supercritical water has been limited to the electric conductivity measurement.[17–22] The recent progress in supercritical water reactions increases the necessity of our understanding of the translational dynamics of neutral molecules, such as water and organic molecules, that cannot be observed by electric conductivity. A widely applicable apparatus for the diffusion measurement in supercritical water is desired to be developed. This is challenged by developing a high-temperature NMR probe. The new probe is multinuclear and can be used for different nuclear species over a wide range of frequencies in a single setup; various metallic elements (ions) can be also observed by the new probe.

We have developed a high-temperature multinuclear diffusion NMR probe in order to elucidate the dynamics of hot water including supercritical. In the previous high-temperature probe,[23,24] the sample was heated by flowing nitrogen gas that is not a good heat conductor. The temperature inhomogeneity in the sample can cause a convection problem. Unless the temperature inhomogeneity is minimized, the convection effect leads to an erroneously large value. Thus, the convection should be reduced as much as possible. In order to overcome the temperature inhomogeneity problem, here we have introduced a new heating and temperature-regulating system; the sample is symmetrically heated from the upper and lower sides by using a solid-state material of high thermal conductivity.

In recent years, we have investigated the hydrogen-bonding structure in super- and subcritical water by applying high-temperature NMR spectroscopy.[23–26] The number of hydrogen bonds per molecule has been determined by combining the experiment on the proton chemical shifts[24] with the molecular-dynamics (MD) simulation.[25] It decreases from ~4 for ambient water to 1–2 but not to zero at 400 °C and in the vicinity of the critical density (0.322 g/cm^3). In addition to the static NMR information, we have obtained the ^{2}H spin-lattice relaxation time for the heavy water in order to determine the rotational time scale (several tens of femtoseconds) in supercritical water over a wide range of density.[26]

[a)]Author to whom correspondence should be addressed. Electronic mail: nakahara@scl.kyoto-u.ac.jp

For understanding the mechanism and dynamics of supercritical water reactions, it is necessary to investigate the molecular translational diffusion as well as the solvation in supercritical water. In this work, we have attempted to elucidate (1) how the self-diffusion coefficient of water depends on the thermodynamic state, (2) how much the $^1H/^2H$ isotope effect on the self-diffusion coefficients is sensitive to the temperature and density in light (^1H_2O) and heavy (^2H_2O) water, and (3) how the simple hydrodynamic model breaks down in sub- and supercritical water.

There have been carried out a few pulsed-field-gradient spin-echo (PGSE) experiments on the self-diffusion coefficient of water in sub- and supercritical water. The results for the self-diffusion coefficient thus obtained at high temperatures scatter from one paper to another. The high-temperature self-diffusion coefficient for light water was previously measured at one-order-of-magnitude lower frequencies, at 28 MHz by Hausser *et al.* (±10% error, $T < \sim 374$ °C),[27] at 21 MHz by Krynicki *et al.* (±5% error, $T \leqslant 225$ °C),[28] and at 60 MHz by Jonas and co-workers (±10% error, 400 °C$\leqslant T \leqslant$700 °C).[29] For heavy water (^2H_2O), it was measured at ~10 MHz only up to 200 °C in a precision of ±5% to ±10% by Jonas and co-workers[30] Thus, the large experimental error has not allowed one to discuss such subtle effect as the isotope effect at high temperatures. The high-temperature probe developed in the present work is operated with a high-field superconductor magnet of 11.3 T (500 and 77 MHz, respectively, for ^1H and ^2H) and the isotope effect can now be studied quantitatively.

The self-diffusion coefficient for water at high temperatures has been interpreted[27–30] in terms of the well-known hydrodynamic relationship (Stokes-Einstein-Debye continuum model) for a particle diffusion; the self-diffusion coefficient (D) divided by the temperature (T) is inversely proportional to the solvent viscosity (η). The standard hydrodynamic model is constructed on the basis of the solute exclusion volume effect (repulsive solute-solvent interactions) and does not explicitly take attractive solute-solvent interactions into account. Attractive interactions play a key role in the density and temperature dependence of D since the hydrogen bonding depends strongly on the thermodynamic state. Previously, we studied the effect of the attractive interactions by scrutinizing the limitations of the hydrodynamic model from the NMR experiments on the dynamics of solitary water in organic solvents[31–33] and benzene in water[34–36] at room temperature. In the literatures on self-diffusion in sub- and supercritical water,[27–30] it has been often assumed that the hydrodynamic model is valid for hot water with $D\eta/T$, the quantity proportional to the inverse effective hydrodynamic radius, almost constant. Although a decrease in the value of $D\eta/T$ with increasing temperature (decreasing density) has been suggested for heavy water,[30] the tendency has been ascribed simply to the experimental uncertainty.[29] In the present study, we confirm the decrease in $D\eta/T$ in a low-density region. Since our experimental uncertainty is much smaller as referred to above, we can elucidate the limitations of the sphere-in-continuum model in a reliable manner. Here we discuss to what extent the translational dynamics in supercritical water is liquidlike or gaslike.

In the following section, we show the design and the performance of the new high-temperature multinuclear diffusion probe. In Sec. III, the procedures for the high-temperature NMR diffusion measurement and the accompanying MD simulation are described. In Sec. IV, the self-diffusion coefficients of light and heavy water are shown and discussed in terms of the experimental reliability, the isotope effect, and the hydrodynamic model. Conclusions are given in Sec. V.

II. HIGH-TEMPERATURE NMR PROBE

A. Apparatus

We have improved the following limitations of the high-temperature NMR probe used previously for supercritical water:[23,24] (1) the field strength of the superconductor magnet was 6.35 T (270 MHz for ^1H, wide bore); (2) the probe was not for multinuclear use (a different probe for each nucleus); and (3) the temperature homogeneity was insufficient for diffusion measurements because of the one-way flow of the heated nitrogen gas from the bottom. The new probe is developed in cooperation with an instrument company (JEOL) and built into a 500 MHz system (JEOL ECA500) with a wide-bore superconductor magnet (11.3 T). The new high-temperature probe is multinuclear and can cover a wide range of resonance frequencies of 36–500 MHz; ^{14}N, ^{35}Cl, ^{133}Cs, ^{17}O, ^2H, ^{29}Si, ^{13}C, ^{23}Na, ^{31}P, ^{19}F, and ^1H can be measured with a single probe.

In Fig. 1, we illustrate the cross-section view of the new high-temperature probe. To minimize the temperature gradient in the sample, two heaters (I, Q) are placed on the upper and lower sides of the sample. For the reduction of the temperature distribution, the sample holder (H) is made of a good heat conductor, a ceramic (aluminium nitride, Yugyokuen Ceramics AlN-200); the high thermal conductivity is 200 W m^{-1} K^{-1}, which is close to that of aluminium (240 W m^{-1} K^{-1}). The ceramic is hard and serves also as a protector for the probe assembly in case of the explosion of the inelastic tube due to a high pressure. The rf coils for high frequency (C), low frequency (D), and field-gradient coils (K) are placed between the triple-layered ceramic coil bobbins (A). Thus, we can place the rf coils closer to the sample and install the gradient coils for a stronger magnetic-field gradient. The rf coils are made of gold and can resist high temperatures up to 450 °C. The coil bobbins also serve as a heat insulator instead of the vacuum double tube used previously. A large magnetic-field gradient of 270 G/cm can be generated at maximum. Hence the probe can be applied for the diffusion measurement of a species with low frequency and/or slow motion. Air (E) and water (F) are circulated for cooling around the gradient coils and the detection circuits, respectively. In order to inhibit the radiant heat from affecting the detection circuit, the silver mirror (M) is placed outside the coil bobbins. To cancel the leaking of the gradient

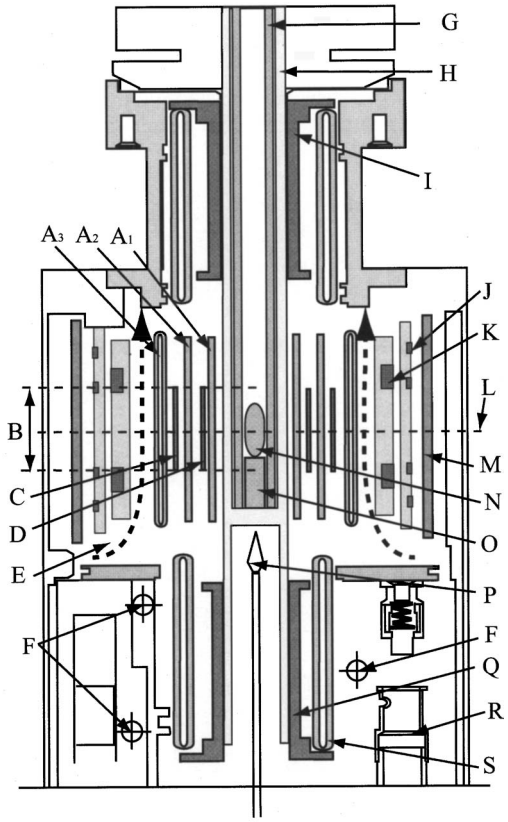

FIG. 1. The cross-section view of the high-temperature multinuclear diffusion NMR probe. (A) Heat insulating tube/coil bobbin for (A_1) the low-frequency rf coil, (A_2) the high-frequency rf coil, (A_3) the fg (field gradient) coil, (B) rf coil length, (C) high-frequency rf coil, (D) low-frequency rf coil, (E) cooling air, (F) cooling water, (G) zirconia tube, (H) sample holder, (I) upper heater, (J) shielding coil, (K) fg coil, (L) rf center, (M) silver mirror for reflecting radiant heat, (N) sample tube, (O) glass spacer, (P) thermocouple, (Q) lower heater, and (R) multinuclear stick holder, and (S) heat insulator.

pulses, the shielding coil (J) is incorporated. The temperature is monitored by the thermocouple (P) placed just below the sample holder.

The present measurements are carried out under isochoric conditions. The high-temperature and high-pressure conditions are controlled by the sealed tube method as described in previous papers.[23,24,26] The sample was sealed in a quartz tube (N) as shown in Figs. 2 and 3. The sealed quartz tube was placed on a glass spacer (O) and positioned to the rf center (L). At temperatures higher than 250 °C, we inserted a zirconia tube (G) between the quartz tube and the sample holder for the protection.

The pressure of water at a supercritical temperature of 400 °C is determined from the *PVT* data recommended by International Association for the Properties of Water and Steam (IAPWS).[37] In this paper, we express the density with the normalized one ρ_n; ρ_n is the density at the state of interest divided by the ambient one. In supercritical conditions, ρ_n is equal to the filling factor defined as the volume ratio of the ambient water to the bore volume of the tube. The accuracy of the ρ_n value is important because of the strong density dependence of the self-diffusion in supercritical water. In this study, ρ_n is determined to an accuracy of 1% as described below. The density of supercritical water can be precisely

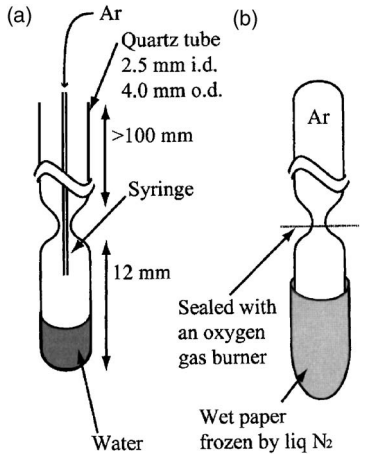

FIG. 2. The preparation of the sample tube; (a) Ar substitution and (b) tube sealing. Details are described in the text.

controlled even in the pressure range close to the critical; recall the difficulty of the pressure-variable method.

The ρ_n is determined after the diffusion measurement. The ρ_n is given by the water volume in a sample tube (2.5 mm i.d. and 4.0 mm o.d.) divided by the bore volume of the tube determined by the inner diameter. The volume of water was obtained by the masses of the tube with and without the sample water. These masses were measured, respectively, before and after the sample water was removed from the quartz tube through a hole made with an oxygen gas burner. The bore volume of the tube is the difference between the total volume of the tube and the volume of the quartz itself; the total volume is the volume determined by the outer diameter and is equal to the sum of the bore volume and the volume of the quartz itself. The total volume of the tube was determined by the change in the position of the meniscus when it was immersed into liquid acetone con-

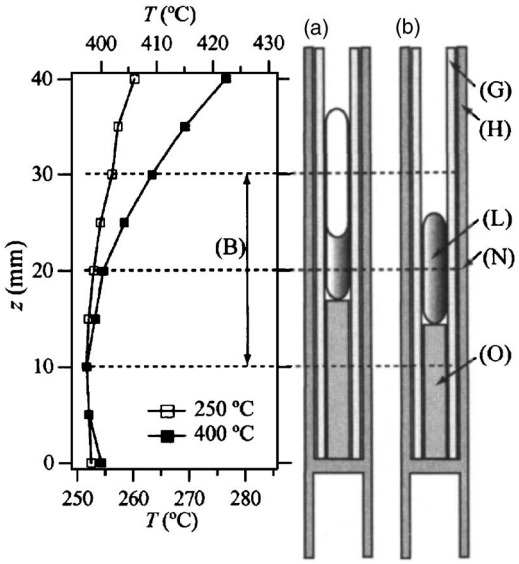

FIG. 3. The temperature distribution in the sample holder as a function of the height z (millimeter) from the bottom; the temperature monitored by the probe thermocouple is 250 °C (open square) and 400 °C (closed square). The sample settings for (a) subcritical and (b) supercritical conditions are shown on the scale corresponding to the longitudinal axis of the graph. The capital letters represent the same components as those in Fig. 1.

tained in a highly uniform NMR tube (5.0 mm o.d.) before the water inside was removed. The volume of the quartz itself was determined by its mass and density data.

The error of the ρ_n for supercritical water is controlled mainly by the total volume of the quartz tube. The increase in the liquid acetone length was ~10 mm and was measured by using a vernier caliper to an accuracy of 1%. The quartz tube and the sample water inside were ~200 mg and several milligrams, respectively. The masses were measured to an accuracy of 1.0 μg using an ultramicrobalance (Mettler Toledo UMX-2); the mass uncertainty is less than 0.1%.

B. Temperature homogeneity

Homogeneous temperature distribution is indispensable for accurate NMR diffusion measurements, particularly at high temperatures. The temperature distribution in the new probe system is shown in Fig. 3 as a function of the height z from the bottom of the sample holder. The temperature distribution has a shallow minimum in the region of the rf center because of the symmetric heating from both the upper and the lower sides. Thus the sample tube is positioned near the temperature minimum. The temperature inhomogeneity is smaller at lower temperatures.

To take advantage of the homogeneous temperature distribution in the probe mentioned above, it is also important to control the size and shape of the sample tube within the space region covered by the rf coils. We should make the sample tube long enough to optimize the shim currents according to the ^{1}H or ^{2}H signals. The length of the quartz tube was taken to be 20 and 12 mm for subcritical and supercritical water, respectively; these are the upper and lower bounds of the tube length. Under the conditions of the coexistence of the liquid and gas phases, the meniscus exists as shown in Fig. 3(a), perturbing the local magnetic field in the sample. The expansion of water at a high temperature can be calculated from the initial volume of ambient liquid water and from that of steam in the sample tube via the filling factor. The relevant *PVT* data are available in literature.[37] For experiments below 350 °C, the sample water is set to be ~7 mm high at room temperature, ~1/3 of the total length of the tube (20 mm); the liquid height is in the range of 7–10 mm at 30–350 °C. In this setup, the sample height is to be fully covered by the rf coil (20 mm high).[38] For experiments at a supercritical temperature of 400 °C, the fluid and the quartz tube are equally 12 mm long as shown in Fig. 3(b); water exists in a single phase. In order to check the reproducibility of the self-diffusion coefficient, the measurement along the coexisting curve has been repeated five times by remounting five different sample tubes (25 runs in total). The uncertainty caused by the sample resetting, that is, an unavoidable uncertainty factor possibly due to the change in the heat conduction condition, is only ±1% up to 350 °C, as shown in Table I. Thus a high reproducibility has been established by improving the temperature homogeneity in the sample.

The currents of upper and lower heaters are adjustable independently to avoid the gravity effect due to the density difference in the vertical direction. We can control the location of the temperature minimum by tuning the currents of the two heaters. Here we set the upper and lower heater currents at 3.20 and 2.60 A, respectively, in order to make the temperature gradient slightly upward with increasing z. This temperature gradient makes the density gradient downward with increasing z, thus the convection along the z axis is hindered by the density gradient. In the previous probe, the temperature gradient was inevitably downward because of the heated gas flow from the bottom of the sample. We can confirm the absence of the convection effect by changing the values of Δ, the time required for water molecules to diffuse in the pulsed-field-gradient spin-echo experiment, over a

TABLE I. The self-diffusion coefficients for light and heavy water determined by (a) NMR experiment and (b) MD simulation in high-temperature conditions including supercritical ones.

		$D(10^{-9}$ m^2 s$^{-1})$[c]	
(a)	T(°C)/ρ_n[a,b]	^1H_2O	^2H_2O
	30/1.000	2.61±0.05	2.06±0.05
	45/0.995	3.52±0.04	2.84±0.04
	60/0.987	4.52±0.06	3.72±0.07
	80/0.976	5.97±0.14	5.01±0.10
	100/0.963	7.67±0.08	6.41±0.10
	125/0.943	9.98±0.26	8.51±0.12
	150/0.921	12.8±0.1	10.9±0.2
	175/0.896	15.8±0.1	13.5±0.1
	200/0.869	18.6±0.4	16.5±0.1
	225/0.837	22.2±0.5	19.6±0.2
	250/0.802	25.8±0.5	23.0±0.4
	275/0.762	29.6±0.8	27.7±0.4
	300/0.715	34.8±0.1	32.0±0.6
	310/0.693	36.5±0.1	34.3±0.2
	320/0.670	38.6±0.1	36.6±0.5
	330/0.644	41.1±0.2	39.1±0.3
	340/0.613	43.9±0.2	41.5±0.2
	350/0.577	46.9±0.3	44.0±0.5
	400/0.251	125±6	⋯
	400/0.230	⋯	137±7
	400/0.206	⋯	134±7
	400/0.170	191±10	⋯
	400/0.131	⋯	278±13
	400/0.088	⋯	316±16
	400/0.071	466±23	⋯
(b)	30/1.00	2.63±0.04	2.26±0.09
	100/0.96	8.46±0.06	7.31±0.18
	150/0.92	13.0±0.1	11.7±0.1
	200/0.87	18.9±0.1	16.9±0.1
	250/0.80	25.0±0.2	22.2±0.2
	300/0.71	34.4±0.2	31.4±0.2
	350/0.58	51.6±0.2	47.2±0.2
	400/0.40	85.3±0.6	77.9±0.1
	400/0.30	115.2±0.4	106.0±0.7
	400/0.20	169.8±0.9	159.3±1.0
	400/0.10	324.3±1.4	306.3±0.9
	400/0.07	441.6±4.4	412.9±2.2

[a] ρ_n is the relative density at the thermodynamic state of interest normalized by the liquid density at 30 °C.
[b] The liquid branch of the saturation curve, except for those at a supercritical temperature of 400 °C.
[c] The error for (b) is expressed at 95% confidence level.

wide range allowed by the large field gradient; see the equation in Sec. III A. The larger the effect of the convection is the larger the apparent diffusion coefficient is; the convection effect is larger for a longer diffusion time Δ. Even when the Δ value was varied from 6.0 to 13.0 ms at 400 °C, the $D(^1H_2O)$ values at ρ_n of 0.170 agreed within 2%. Thus the convection effect is negligibly small in this work.

The sample temperature was stable over time within ±0.2 °C in the temperature range studied; this is due to the feedback on the temperature control. The temperature was monitored by means of a thermocouple made of platinum and platinum-rhodium placed below the sample holder. A calibration curve (almost linear) was established between the temperature at the center of the rf coil (z=20 mm) and the temperature monitored by the thermocouple below the sample holder. The sample temperature was controlled using the pulsed direct current applied at an on/off interval of 2.4 s. In order to avoid noises from the current on/off, the heater switches were left untouched, either in on or off mode, during the acquisition of each free-induction decay (FID), switched on at temperatures higher than 250 °C, and switched off at lower temperatures. The FID acquisition was typically ~4 s for both ^1H and ^2H.

III. PROCEDURES

A. Diffusion measurement

Light water (^1H_2O) was purified using a Milli-Q Labo (Millipore) filter system. Heavy water (^2H_2O; 99.9% ^2H purity) was obtained from CEA (Commissariat a L'Enegie Atomique, France) and used without further purification. To remove the paramagnetic oxygen, the air inside was exchanged by argon using a syringe before the quartz tube was sealed with an oxygen gas burner as in Fig. 2. The quartz tube was narrowed in the middle like an hourglass before water was introduced. The tube was sealed after the sample water was frozen by liquid nitrogen; the tube end was wrapped with a wet paper during the sealing.

The diffusion coefficient is obtained by the pulsed-field-gradient spin-echo method. The sequence of the signal intensities is fitted to[39,40]

$$A(\Delta,\delta) = A(\Delta,0)\exp\left\{-\gamma^2 g^2 D\delta^2\left(\frac{4\Delta-\delta}{\pi^2}\right)\right\}. \quad (1)$$

Here, $A(\Delta,\delta)$ and $A(\Delta,0)$ are the intensities of the spin-echo signal when the field gradient is present and absent, respectively; γ is the magnetogyric ratio; D is the self-diffusion coefficient, g is the intensity of the half-sine-shaped magnetic-field gradient; δ is the duration of the magnetic-field-gradient pulse; Δ is the time interval between the two gradient pulses, corresponding to the time required for water molecules to diffuse. The field gradient was calibrated by the use of the known self-diffusion coefficient of light water; $D=2.61\times10^{-9}$ m^2 s^{-1} at 30 °C.[41,42] The diffusion coefficient is measured by varying δ and fixing the values of Δ and g. In each measurement, we took 20 different values of δ.

To check the reproducibility, the measurement along the coexisting curve was repeated five times for five different samples at each temperature below 350 °C; it took at most

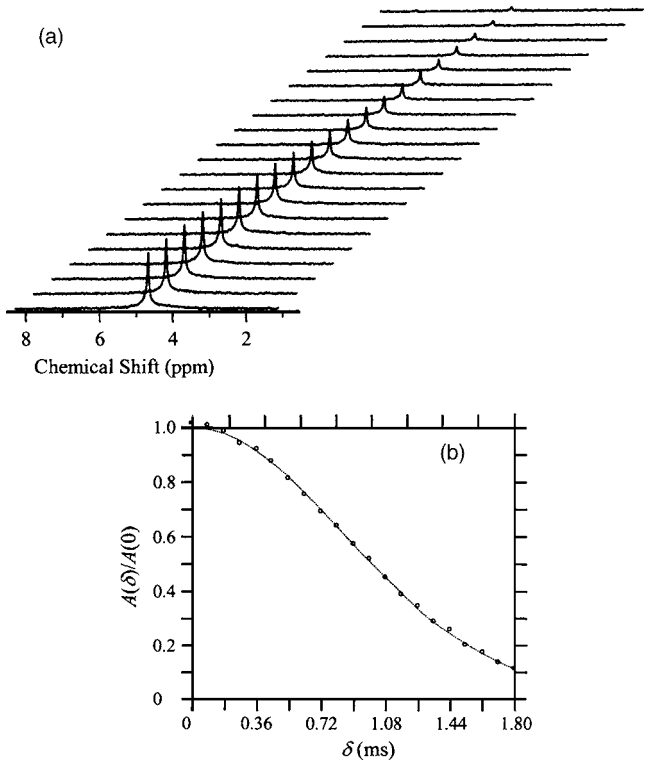

FIG. 4. (a) The attenuation of the echo signal of ^2H in ^2H_2O with a density of ρ_n=0.088 and a supercritical temperature of 400 °C. (b) The intensity of the echo signals shown in (a) as a function of the duration of the magnetic-field-gradient pulses δ. The sequence of the signal intensities are fitted to Eq. (1). The g and the Δ are 49.9 G/cm and 13 ms, respectively. The signal intensities are arbitrary.

30 min to reach the equilibrium temperature after an increase of 25 °C.[43] The uncertainty of D is ±0.5% in repeated measurements for a single sample and the total uncertainty is ±1% as shown in Table I. At 400 °C, the uncertainty is ±1% among five runs consecutively performed for one sample. The total uncertainty of D at 400 °C is estimated at about ±5% by taking into account the error due to the sample resetting. The small uncertainty indicates the stability of temperature and the reproducibility of gradient pulses in this experiment.

The quality of our multinuclear spectra can be seen from those in Fig. 4(a) taken under extreme conditions. There are shown the ^2H spectra for heavy water at a low density of ρ_n=0.088 at a supercritical temperature of 400 °C. This is the most difficult condition for the acquisition of the FID signals in this work. The FID signals were accumulated once for each δ. The signal-to-noise ratio for δ=0 ms exceeds 40, resulting in accurate diffusion coefficients within ±1%. The intensities of spin-echo signals $A(\Delta,\delta)$ are extracted from Fig. 4(a) and plotted in Fig. 4(b) as a function of the duration time δ in order to determine the diffusion coefficient.

B. Molecular-dynamics simulation

The molecular-dynamics simulation was performed for both light (^1H_2O) and heavy (^2H_2O) water to obtain their self-diffusion coefficients D for comparison with experiment. The TIP4P-FQ model was adopted as the potential function.[44] The molecular-dynamics simulation was per-

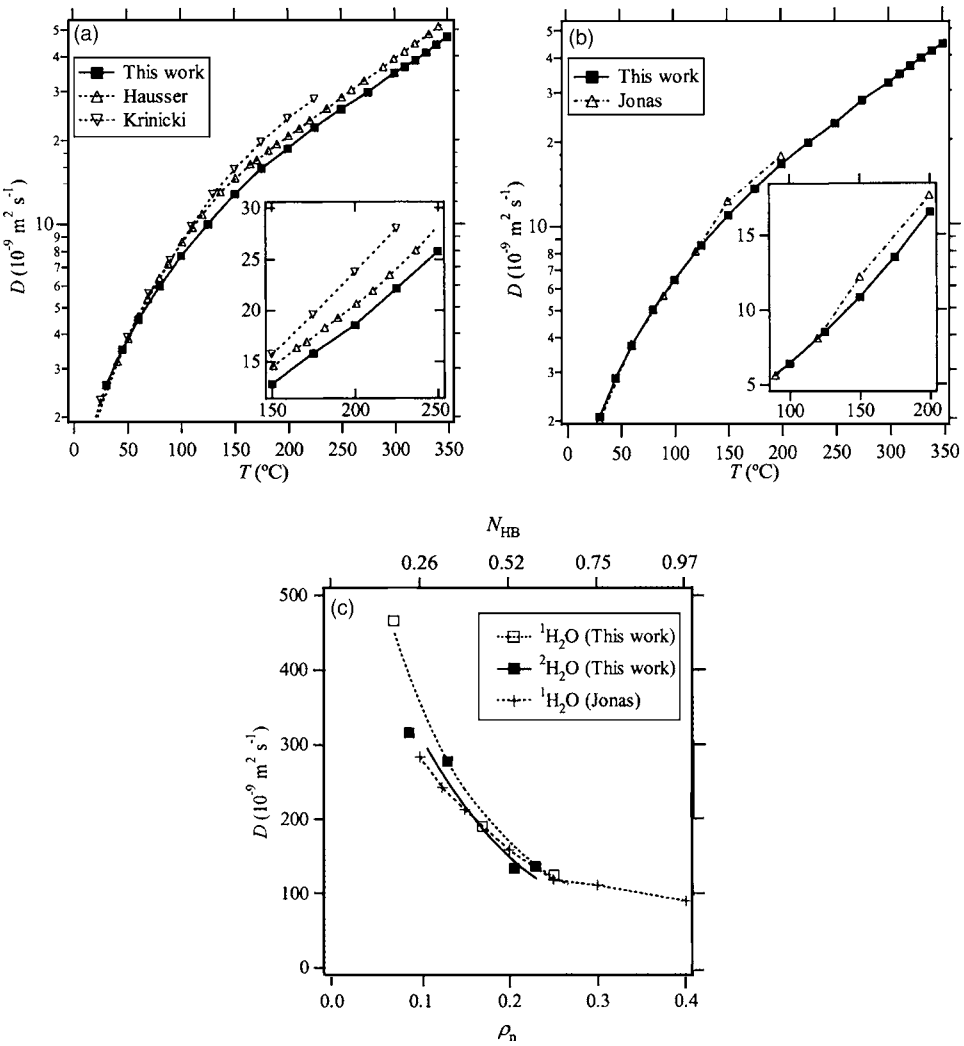

FIG. 5. The self-diffusion coefficients of water determined; (a) $D(^1H_2O)$ and (b) $D(^2H_2O)$ plotted against the temperature along the liquid-gas coexisting curve, and (c) $D(^1H_2O)$ and $D(^2H_2O)$ against the density at 400 °C. The literature values are obtained by Hausser *et al.* (Ref. 27) and Krynicki *et al.* (Ref. 28) (a), by Jonas and co-workers (Ref. 30) (b), and by Jonas and co-workers (Ref. 29) (c). The N_{HB} in (c) indicates the average number of hydrogen bonds in which a water molecule is involved, as determined by the present MD simulation.

formed using a time-reversible quarternion algorithm.[45] The simulation procedure was the same as that described in Ref. 26. The molecular dynamics was carried out for 1 ns at each state of interest. The thermodynamic conditions covered by the simulation is on the liquid branch of the liquid-gas coexistence curve from 30 to 350 °C and supercritical states specified by densities of ρ_n=0.07, 0.10, 0.20, 0.30, and 0.40 and a temperature of 400 °C.

IV. RESULTS AND DISCUSSION

A. Self-diffusion coefficients

First we show the reliability of the new high-temperature probe. The self-diffusion coefficients (D) obtained for light (^1H_2O) and heavy (^2H_2O) water are to be compared with those obtained by the tracer method in the ambient temperature range of 30–60 °C.[41,46] The widely accepted D value of 2.61×10^{-9} m^2 s^{-1} is taken here as a reference value for ^1H_2O at 30 °C.[41] In the low-temperature range, the present values are in good agreement with those in literature. In the case of ^1H_2O, for example, the present values of 3.52×10^{-9} m^2 s^{-1} at 45 °C and 4.52×10^{-9} m^2 s^{-1} at 60 °C are in conformity with the corresponding values of 3.58×10^{-9} m^2 s^{-1} by Mills[41] and 4.70×10^{-9} m^2 s^{-1} by Harris and Woolf.[46] In this multinuclear probe system, it is not necessary to change probes when we observe the self-diffusion coefficients for ^1H_2O and ^2H_2O. The field-gradient calibration is common for ^1H and ^2H. The agreement is excellent between our values and those of related literature for $D(^2H_2O)$ at 30 and 45 °C.[41] Our value is 2.13×10^{-9} m^2 s^{-1} and that of literature is 2.15×10^{-9} m^2 s^{-1} at 30 °C; our value is 2.92×10^{-9} m^2 s^{-1} and that of literature is 3.00×10^{-9} m^2 s^{-1} at 45 °C.

Now let us see the D values at higher temperatures. The D values determined for ^1H_2O and ^2H_2O along the coexisting curve are plotted against the temperature in Figs. 5(a) and 5(b), respectively, together with the literature values.[27,28,30,47] The D values for ^1H_2O by Hausser *et al.*[27] are larger by ~10% (their uncertainty) than the present over the entire temperature range. The D values for ^1H_2O by Krynicki *et al.*[28] are ~20% larger; the difference exceeds their experimental uncertainty (±5%). The difference can be ascribed to the convection effect in their apparatus.[48–50] For the case of ^2H_2O, the D values of Jonas and co-workers[30] are in reasonable agreement with the present values [see Fig. 5(b)].

Under supercritical conditions, there are no D values reported except for $D(^1H_2O)$ by Jonas and co-workers[29] Recent computer simulation methods, which are dramatically improved in reproduction of experimental results,[51–57] can be

used to compare the overall profiles of the self-diffusion coefficients observed using the new probe. As seen from Table I, the D values by the NMR experiment and the MD simulation agree fairly well over a wide density range.[58,59] In the previous paper,[26] the values of τ_{2R} obtained by our NMR measurements and the TIP4P-FQ model agreed excellently. The present agreement between the experiment and the MD simulation is in favor of the reliability of the new high-temperature NMR probe.

The temperature and density effects are not separated when the temperature is varied along the saturation curve. In supercritical water, however, the density effect can be isolated by fixing the temperature; thus the kinetic and potential effects are more clearly differentiated. In Fig. 5(c), we show $D(^1H_2O)$ and $D(^2H_2O)$ determined by the NMR experiment at 400 °C as a function of water density ρ_n. Our D values agree with those by Jonas and co-workers[29] within their error. The self-diffusion coefficient increases weakly with decreasing density down to 0.2 g/cm^3 and increases more rapidly below 0.2 g/cm^3. The present MD simulation shows that the number of hydrogen bonds in water at 400 °C is 0.96, 0.74, 0.52, 0.26, and 0.18, respectively, at 0.4, 0.3, 0.2, 0.1, and 0.07 g/cm^3; note that hydrogen bonds still persist even at such low densities at 400 °C. Roughly speaking, the observed self-diffusion coefficient of supercritical water appears, although not exactly, inversely proportional to the density or the number of hydrogen bonds in the low-density region covered in this study. The proportionality that is predicted in the zero-density limit by the simple gas kinetic theory[60] was indeed pointed out in the previous paper.[29]

B. ^{1}H/^{2}H isotope effect

One of our motivations is to observe the dynamic isotope effect on the self-diffusion of water over a wide range of density and temperature. In ambient conditions, the diffusion data of various isotopic species of water have yielded a rather detailed picture on the diffusion in water.[61,62] There have also been recent developments of computer simulations which treat the isotope effect in some detail.[63–65] In spite of the recent increase of interest in the dynamic isotope effect in water, reliable data are still awaited at high temperatures and high pressures, owing to experimental difficulties. The isotope effect is much smaller than the density and temperature effects so that high accuracy is required. The new high-temperature probe developed here is powerful enough to determine the isotope effect on water diffusion at high temperatures.

It is predicted by the gas kinetic theory[60] that, in the zero-density limit, the $D(^1H_2O)/D(^2H_2O)$ is equal to the square root of the mass ratio $(m(^2H_2O)/m(^1H_2O))^{1/2}$, 1.05. It is then natural to predict that the isotope ratio of $D(^1H_2O)/D(^2H_2O)$ approaches 1.05 when the density is low enough. Contrary to the prediction above, the isotope ratio $D(^1H_2O)/D(^2H_2O)$ obtained using the previous values[27,30] is constant or even increases with increasing temperature on the saturation curve. Here we investigate how the isotope ratio depends on temperature and density.

In Fig. 6, we plot the isotope ratio $D(^1H_2O)/D(^2H_2O)$ against the temperature along the coexisting curve. It is clearly shown that the isotope effect depends on temperature and density. The isotope ratio decreases with increasing temperature. The value $D(^1H_2O)/D(^2H_2O)$, which is 1.23 in ambient water, becomes close to and slightly larger than unity at 350 °C. The above-mentioned constant or increasing isotope effect comes from the larger D value used for ^1H_2O.[27,28] The decreasing isotope effect is in fair agreement with our MD simulation. It is to be noted that the present MD simulation is classical and cannot determine all the isotope effect. The quantum effect is reported to increase the diffusivity of water molecules.[65] The isotope ratio $D(^1H_2O)/D(^2H_2O)$ taken elsewhere[65] is almost constant from room temperature to high temperature, contrary to the present experimental result. A more detailed analysis of the density dependence and the molecular mechanism will be discussed in a forthcoming paper on supercritical water.

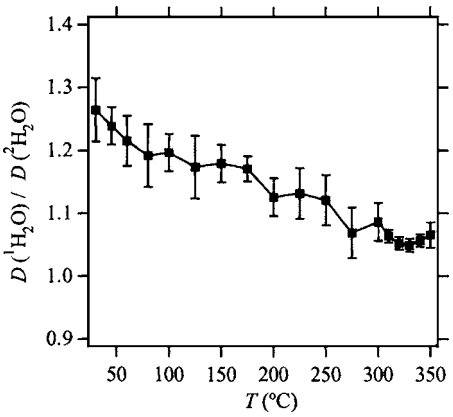

FIG. 6. Temperature dependence of the isotope ratio $D(^1H_2O)/D(^2H_2O)$ along the liquid branch of the liquid-vapor coexisting curve.

Since ^2H_2O is considered to be more structured than ^1H_2O,[26,66,67] the isotope effect is interesting to discuss in terms of intermolecular interaction, typically hydrogen bonding, apart from the density and the temperature dependences. In ambient conditions, the effect of intermolecular interaction strength overwhelms the mass effect; the lower the temperature and/or the higher the density is, the larger the isotope effect is.[68,69] It is known that the replacement of ^1H by ^2H causes a larger difference in the self-diffusion of water than does the replacement of ^{16}O by ^{18}O; the $D(^2H_2O)$ is 20% smaller than $D(^1H_2O)$ in ambient conditions,[41] while the D for $^1H_2{}^{18}O$ is only 5% smaller than that for $^1H_2{}^{16}O$.[46] It is of great interest to investigate the effect of the weakened and distorted hydrogen bonding on the self-diffusion for super- and subcritical water from the classical and quantum mechanical points of view.

C. Test of the Stokes-Einstein-Debye law

In previous works,[27–30] there has been discussions of the applicability of the simple hydrodynamic (Stokes-Einstein-Debye) model for the self-diffusion coefficient of hot water at densities higher than the critical (0.322 g/cm^3). The simple hydrodynamic expression for the self-diffusion coef-

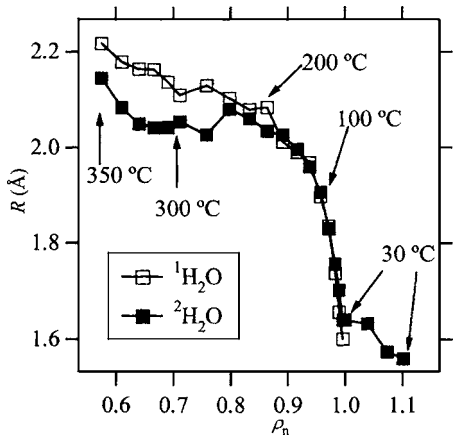

FIG. 7. Plots of the effective hydrodynamic radius R for ^1H_2O and ^2H_2O against the normalized density ρ_n. The boundary condition parameter f is set to 4 (slip boundary condition). The R for ^2H_2O at higher densities than 1.0 is calculated from the D and η in Refs. 74 and 75, respectively.

ficient D is based on the sphere-in-continuum model and expressed in terms of the macroscopic solvent viscosity η divided by the temperature T as

$$D = \frac{k_B}{f\pi R}\frac{T}{\eta}, \tag{2}$$

where k_B is the Boltzmann constant, f is the boundary condition parameter, equal to 4 for the slip boundary condition and 6 for the stick, and R is the effective radius of the diffusing species. The recommended data on η are available in literature.[70–72] Here we take the slip boundary condition ($f=4$) because the stick one ($f=6$) gives us an unphysically small radius for water. For the case of $f=4$, the R value at an ambient condition is closer to the commonly accepted radius of water, 1.4 Å. The validity of the standard hydrodynamic model is tested here for $f=4$ in a more reliable way than before[27–30] with the aid of the more comprehensively determined data for expanded hot water.

The R values for light and heavy water have been obtained by applying Eq. (2) to the self-diffusion coefficients from our NMR measurements. The R is plotted against the water density in Fig. 7. The ambient values of R for ^1H_2O and ^2H_2O are equal to 1.6 Å, larger than the molecular radius, 1.4 Å, probably due to attractive interactions. In contrast to the previous results,[27–30] the R is not constant but dramatically *increases* with decreasing density above $\rho_n=0.92$(<150 °C), and the increasing rate becomes much weaker at the higher temperatures. The R increases from 1.6 to 2.0 Å as the density ρ_n decreases from 1.00 (30 °C) to 0.80 (250 °C). The increase of the effective hydrodynamic radius can be interpreted as an indication of the strong effect of the short-range attractions between the solute (water)-solvent (water). A similar tendency of the R has been observed when the attractive solute-solvent interactions are increased in the case of the solitary water in various organic solvents.[33] When the $1/D$ (proportional to R) is plotted against η/T (hydrodynamic plot), the slope is not invariant but increases as the water density drops with increasing temperature along the liquid-vapor coexisting curve. It is to be noted that the increase in R with decreasing density has also been observed for compressed water at high densities of $\rho_n=1.0-1.1$ at 30 °C.[73] This is because the increase[74] in D overwhelms the decrease[75] in η when hydrogen bonds are weakened and distorted by compression; D is a single-molecular property, while η is collective. The density dependence of the R in the thermal *expansion* is much larger than that in the *compression* at a fixed temperature, probably due to the additional kinetic effect. In general, the R increases when ρ_n decreases at the high molecular packing density in the vicinity of $\rho_n=1.0$. In supercritical conditions, the effective radius R dramatically decreases with decreasing density, as previously stated,[29] the R for ^1H_2O falls to 0.46 from 2.35 Å as ρ_n decreases from 0.251 to 0.071. Thus the continuum hydrodynamic model is invalid for water, hydrogen-bonding system, in a quantitative sense.[76]

The newly obtained values $D(^2H_2O)$ at 400 °C enables us to compare the density dependence of translational and rotational dynamics in supercritical water. The translational diffusion depends on the density of supercritical water much more strongly than does the rotational correlation time $\tau_{2R}(^2H_2O)$. The value $D(^2H_2O)$ increases by a factor of 2.3 as the water density ρ_n decreases from 0.230 to 0.088, while $\tau_{2R}(^2H_2O)$ increases only by 10% as ρ_n decreases from 0.3 to 0.1. In this density region, the water is mostly in the monomer or dimer state. When a water molecule translationally diffuses, it must go out of the potential well, and the density effect on the translational mobility can be large. On the other hand, when a water molecule rotates, the rotational potential barrier would be much smaller.

V. CONCLUSIONS

The high-temperature multinuclear diffusion NMR probe has been newly developed for the superconductor magnet of 11.3 T (500 MHz for ^1H). Using the new high-temperature probe, we have determined in high precision the self-diffusion coefficients D for light (^1H_2O) and heavy (^2H_2O) water at 30–350 °C on the liquid-vapor coexisting curve and at 400 °C and 0.071–0.251 g/cm^3. The D for water is determined to an accuracy of ±1% and ±5% in sub- and supercritical conditions, respectively. The D values obtained by the present experiment are in fair agreement with those obtained by the MD simulation over a wide density range, in favor of the reliability of our new measurement. The results obtained are summarized as follows.

(1) The D increases with increasing temperature and decreasing density.
(2) The ratio $D(^1H_2O)/D(^2H_2O)$ decreases from 1.23 to ~1.0 with increasing temperature from 30 to 400 °C.
(3) The hydrodynamic radius R obtained by simple hydrodynamic model increased with decreasing density on the liquid-vapor saturation curve and decreased with decreasing density in supercritical conditions.

The decrease of the isotope ratio $D(^1H_2O)/D(^2H_2O)$ with increasing temperature is in fair agreement with the present MD simulation. The hydrodynamic (Stokes-Einstein-Debye) model is invalid over the entire thermodynamic state covered in this study, necessitating a new molecular ap-

proach to the self-diffusion in hydrogen-bonding liquid that takes attractive intermolecular interactions into account. We expect that this can be attained by performing a detailed computer simulation.

ACKNOWLEDGMENTS

This work was supported by the Grant-in-Aid for Scientific Research 15205004 from Japan Society for the Promotion of Science and by the Grant-in-Aid for Creative Scientific Research 13NP0201 the Grant-in-Aid for Scientific Research on Priority Area 15076205 and the NAREGI (National Research Grid Initiative) Project from the Ministry of Education, Culture, Sports, Science, and Technology, Japan. We thank Dr. Toshiko Hirano of Kyoto University for technical advices on the measurement of masses of the sample tubes.

[1] *Water, a Comprehensive Treatise*, edited by F. Franks (Plenum, New York, 1972–1982), Vols. 1–7.
[2] J. F. Connolloy, J. Chem. Eng. Data **11**, 13 (1966).
[3] Z. Alwani and G. Schneider, Ber. Bunsenges. Phys. Chem. **71**, 633 (1967).
[4] M. Christoforakos and E. U. Franck, Ber. Bunsenges. Phys. Chem. **90**, 780 (1986).
[5] G. Wu, M. Heilig, H. Lentz, and E. U. Franck, Ber. Bunsenges. Phys. Chem. **94**, 24 (1990).
[6] R. Duel and E. U. Franck, Ber. Bunsenges. Phys. Chem. **95**, 847 (1991).
[7] R. W. Shaw, T. B. Brill, A. A. Clifford, C. A. Eckert, and E. U. Franck, Chem. Eng. News **69**, 26 (1991).
[8] J. W. Tester, H. R. Holgate, F. J. Armellini, P. A. Webley, W. R. Killilea, G. T. Hong, and H. E. Barner, ACS Symp. Ser. **518**, 35 (1993).
[9] J. S. Seewald, Nature (London) **370**, 285 (1994).
[10] F. N. Spiess *et al.*, Science **207**, 1421 (1980).
[11] N. Akiya and P. E. Savage, Chem. Rev. (Washington, D.C.) **102**, 2725 (2002).
[12] M. Watanabe, T. Sato, R. L. Smith, Jr., K. Arai, A. Kruse, and E. Dinjus, Chem. Rev. (Washington, D.C.) **104**, 5803 (2004).
[13] K. Yoshida, C. Wakai, N. Matubayasi, and M. Nakahara, J. Phys. Chem. A **108**, 7479 (2004).
[14] Y. Nagai, S. Morooka, N. Matubayasi, and M. Nakahara, J. Phys. Chem. A **108**, 11635 (2004).
[15] N. Matubayasi and M. Nakahara, J. Chem. Phys. **122**, 074509 (2005).
[16] S. Morooka, C. Wakai, N. Matubayasi, and M. Nakahara, J. Phys. Chem. A **109**, 6610 (2005).
[17] A. S. Quist and W. L. Marshall, J. Phys. Chem. **72**, 684 (1968).
[18] A. Ebertz and E. U. Franck, Ber. Bunsenges. Phys. Chem. **99**, 1091 (1995).
[19] P. C. Ho, H. Bianchi, D. A. Palmer, and R. H. Wood, J. Solution Chem. **29**, 217 (2000).
[20] T. Hoshina, N. Tsuchihashi, K. Ibuki, and M. Ueno, J. Chem. Phys. **120**, 4355 (2004).
[21] L. Hnedkovsky, R. H. Wood, and V. N. Balashov, J. Phys. Chem. B **109**, 9034 (2005).
[22] M. Nakahara, *Proceedings of the 14th International Conference on the Properties of Water and Steam, Kyoto, 29 August–3 September 2004*, edited by M. Nakahara, N. Matubayasi, M. Ueno, K. Yasuoka, and K. Watanabe (Maruzen, Tokyo, 2005), p. 12.
[23] N. Matubayasi, C. Wakai, and M. Nakahara, Phys. Rev. Lett. **78**, 2573 (1997).
[24] N. Matubayasi, C. Wakai, and M. Nakahara, J. Chem. Phys. **107**, 9133 (1997).
[25] N. Matubayasi, C. Wakai, and M. Nakahara, J. Chem. Phys. **110**, 8000 (1999).
[26] N. Matubayasi, N. Nakao, and M. Nakahara, J. Chem. Phys. **114**, 4107 (2000).
[27] R. Hausser, G. Maier, and F. Noack, Z. Naturforsch. Teil A **21**, 1410 (1966).
[28] K. Krynicki, C. D. Green, and D. W. Sawyer, Faraday Discuss. Chem. Soc. **66**, 199 (1979).
[29] W. J. Wilber, G. A. Hoffman, and J. Jonas, J. Chem. Phys. **74**, 6875 (1981).
[30] D. J. Wilbur, T. DeFries, and J. Jonas, J. Chem. Phys. **65**, 1783 (1976).
[31] M. Nakahara and C. Wakai, J. Chem. Phys. **97**, 4413 (1992).
[32] C. Wakai and M. Nakahara, J. Chem. Phys. **103**, 2025 (1995).
[33] C. Wakai and M. Nakahara, J. Chem. Phys. **106**, 7512 (1997).
[34] M. Nakahara, C. Wakai, and N. Matubayasi, J. Phys. Chem. **99**, 1377 (1995).
[35] M. Nakahara, C. Wakai, Y. Yoshimoto, and N. Matubayasi, J. Phys. Chem. **100**, 1345 (1996).
[36] C. Wakai, N. Matubayasi, and M. Nakahara, J. Phys. Chem. A **103**, 6685 (1999).
[37] Release on the IAPWS Formulation 1995 for the Thermodynamic Properties of Ordinary Water Substances for General and Scientific Use, URL: http://www.iapws.org
[38] The influence of the steam phase is negligible in this setup at subcritical conditions for the following reason. The spectrum of the gas phase and liquid phase are separated in chemical shift by 1–4 ppm (Ref. 24), which is much larger than the signal width. Furthermore, since the shim current was optimized for the liquid phase, the gas-phase spectrum does not appear, as shown in Fig. 4(a).
[39] E. O. Stejskal and J. E. Tanner, J. Chem. Phys. **42**, 288 (1965).
[40] P. Stilbs, Prog. Nucl. Magn. Reson. Spectrosc. **19**, 1 (1987).
[41] R. Mills, J. Phys. Chem. **77**, 685 (1973).
[42] In this study, we used the D for light water in neat light water for the magnetic-field gradient calibration. This was possible owing to the absence of the radiation damping effect. Alternatively, the D for impurity light water in neat heavy water at 30 °C (2.19×10^{-9} m^2 s^{-1}) calculated in Ref. 33 can be used.
[43] For the measurement at 100 °C, we raised the temperature up to 125 °C first and gradually cooled down the sample to 100 °C. In this way, we could circumvent the difficulty in measuring the diffusion coefficient at the boiling point. When we simply raised the temperature up to 100 °C from room temperature and measured the diffusion coefficient, the reproducibility was severely worse than at the other temperatures, probably due to the bubbling effect at 100 °C.
[44] S. W. Rick, S. J. Stuart, and B. J. Berne, J. Chem. Phys. **101**, 6141 (1994).
[45] N. Matubayasi and M. Nakahara, J. Chem. Phys. **110**, 3291 (1999).
[46] K. R. Harris and L. A. Woolf, J. Chem. Soc., Faraday Trans. 1 **76**, 377 (1980).
[47] The literature values plotted in Fig. 5 are not corrected by ITS-90. If the D values in Refs. 27–30 are corrected by ITS-90, they become only 2% smaller. Thus, the difference of temperature standards does not affect our arguments even if it is neglected.
[48] In the apparatus used by Krynicki *et al.* described in Refs. 49 and 50, materials of low thermal conductivity are used; titanium alloy (8 W/m K) for the pressure vessel, glass (~0.03 W/m K) for the other parts, and mercury (8 W/m K) for the pressure transmission.
[49] J. G. Powles and M. C. Gough, Mol. Phys. **16**, 349 (1969).
[50] D. W. Sawyer and B. N. Gale, J. Phys. E **6**, 1205 (1973).
[51] H. J. C. Berendsen, J. R. Grigera, and T. P. Straatsma, J. Phys. Chem. **91**, 6269 (1987).
[52] L. X. Dang, J. Chem. Phys. **97**, 2659 (1992).
[53] N. Yoshii, H. Yoshie, S. Miura, and S. Okazaki, J. Chem. Phys. **109**, 4873 (1998).
[54] P. B. Balbuena, K. P. Johnston, P. J. Rossky, and J. K. Hyun, J. Phys. Chem. B **102**, 3806 (1998).
[55] A. A. Chivalo and P. T. Cummings, Adv. Chem. Phys. **109**, 115 (1999).
[56] M. S. Skaf and D. Laria, J. Chem. Phys. **113**, 3499 (2000).
[57] C.-N. Yang and H. J. Kim, J. Chem. Phys. **113**, 6025 (2000).
[58] At ambient condition, the MD simulations for D in water with the TIP4P-FQ model can yield deviations of ~20% from the experimental data as in Ref. 59. At high temperatures, the deviation is 10%–15%, as shown in Table I.
[59] S. W. Rick, J. Chem. Phys. **114**, 2276 (2001).
[60] D. A. McQuarrie, *Statistical Mechanics* (Harper & Row, New York, 1976), Chap. 19.
[61] R. Mills and K. R. Harris, Chem. Soc. Rev. **5**, 215 (1976).
[62] H. Weingärtner, Z. Phys. Chem., Neue Folge **132**, 129 (1982).
[63] Y. Marcus and A. Ben-Naim, J. Chem. Phys. **83**, 4744 (1985).
[64] R. A. Kuharski and P. J. Rossky, J. Chem. Phys. **82**, 5164 (1985).
[65] B. Guillot and Y. Guissani, J. Chem. Phys. **108**, 10162 (1998); Fluid Phase Equilib. **151**, 19 (1998).

[66] G. Némethy and H. A. Scheraga, J. Chem. Phys. **41**, 680 (1964).
[67] M. Nakahara, M. Zenke, M. Ueno, and K. Shimizu, J. Chem. Phys. **83**, 280 (1985).
[68] J. Buchhauser, T. Groß, N. Karger, and H.-D. Lüdemann, J. Chem. Phys. **110**, 3037 (1999).
[69] L. Chen, T. Groß, H. Krienke, and H.-D. Lüdemann, Phys. Chem. Chem. Phys. **3**, 2025 (2001).
[70] Revised Release on the IAPS Formulation 1985 for the Viscosity of Ordinary Water Substance (2003), URL: http://www.iapws.org
[71] Release on Viscosity and Thermal Conductivity of Heavy Water Substance (1984), URL: http://www.iapws.org
[72] The temperature scale in Ref. 71 is revised using the International Temperature Scale of 1990 in order to make the information consistent with those in Ref. 70.
[73] C. Wakai and M. Nakahara, J. Chem. Phys. **100**, 8347 (1994).
[74] L. A. Woolf, J. Chem. Soc., Faraday Trans. 1 **72**, 1267 (1976).
[75] A. Harlow, Ph.D. thesis, London University (1970).
[76] The anomalous density dependence of R due to attractive interactions can be absorbed when the standard hydrodynamic relation [Eq. (2)] is modified conventionally as in Ref. 73 using the fractional power α; $D=(k_B/f\pi R)(T/\eta)^{\alpha}(0<\alpha<1)$. The parameters, α and R, involved have been derived by fitting the self-diffusion data to the above equation; for the case of $f=4$, $\alpha=0.88\pm0.01$ and 0.90 ± 0.01, and $R=1.80\pm0.01$ and 1.85 ± 0.01 Å, for ^1H_2O and ^2H_2O, respectively. When the R is fixed as the above values that are larger than 1.4 Å, the D is inversely proportional to the $(\eta/T)^{\alpha}$ instead of η/T. The R is larger than the molecular radius, 1.4 Å, probably due to the attractive interactions.